Grzegorz KAMIŃSKI, Włodzimierz PRZYBOROWSKI, Paweł STASZEWSKI, Adam BIERNAT, Emil KUPIEC

Warsaw University of Technology

Design and Test Results of Laboratory Model of Linear Induction Motor for Automation Personal Urban Transport PRT

Abstract. In the paper design, exploitation characteristics and results of experimental test of down-scaled Linear Induction Motor (LIM) model is presented. LIM model was scaled by factor 1:4 in respect to nominal parameters and dimensions of full scale drive destined for Automatic Personal Urban Transport – PRT. LIM model was designed according to foundations and dimensional constrains resulting from specification of laboratory track. Within the confines of project several LIM model prototypes were prepared. The calculation algorithms and calculation results on the base of circuit and field methods are discussed. Integral part of project was elaboration of experimental tests procedures and original measurement system that allowed to perform wide range of motor prototypes tests. Proposed measurement system consist of measurement sensors, converters and dedicated system for data acquisition and processing based on the LabVIEW environment. Test range included thermal, driving and normal force measuremenst for variant parameters of voltage, current and frequency signals.

*Streszczenie. W artykule przedstawiona została konstrukcja, charakterystyki eksploatacyjne i wyniki badań eksperymentalnych modelu liniowego silnika liniowego (LIM) w zmniejszonej skali. Zastosowano współczynnik skalowania 1:4 w stosunku do parametrów znamionowych i geometrii pełnowymiarowego napędu przeznaczonego do zastosowań w Automatycznym Osobowym Transporcie Miejskim – PRT. Modelu LIM został zaprojektowany zgodnie z założeniami i ograniczeniem wymiarów wynikającymi ze specyfikacji laboratoryjnego toru jezdnego. W ramach ograniczeń projektowych zrealizowanych zostało kilka prototypowych modeli LIM. Omówione zostały algorytmy obliczeniowa i wyniki obliczeń zrealizowane w oparciu o metody obwodowe i polowe. Integralną częścią projektu było opracowanie procedur pomiarowych oraz system oryginalnego pomiarowego umożliwiającego wykonanie znacznego zakresu badań prototypów silnika. Proponowany system pomiarowy złożony z czujników i przetworników pomiarowych oraz systemu akwizycji i przetwarzania danych wykorzystującego środowisko LabVIEW. Zakres zrealizowanych badań obejmował badania cieplne, pomiary sił ciągu i naciągu dla wariantowych parametrów: napięcia, prądu i częstotliwości. **Konstrukcja, charakterystyki eksploatacyjne i wyniki badań eksperymentalnych modelu liniowego silnika liniowego***

Keywords: LIM, PRT, linear motor design, linear motor test.
Słowa kluczowe: SIL, PRT, projektowanie silników indukcyjnych liniowych, badanie silników indukcyjnych liniowych

Introduction

Reliability of Linear Induction Motors (LIM) drives (directly realizing kinematics of translatory motion) due to elimination of gears in the propulsion system and slip between track and wheels and moreover simplicity of service, maintenance and preservation, designates this kind of drives for automation personal urban transport system (PRT). Among several papers concerning domain of linear electrical motors [1, 2, 3, 4, 5, 6, 12, 17] only comparatively few undertake problem of PRT drive systems. In this area interesting are works of Anderson [1, 2] and Ranky [15] in which authors state the preference of asynchronous motor against synchronous one due to simplicity of construction and reversibility of primary (inductor) and secondary (armature) circuits in the install place (vehicle - track). It is necessary to notice that technological progress in respect to supply systems and carry out of sub-assemblies may affect the economy of PRT system defined by cost in respect to single user and unit of travelling distance.

Summing up one can state:
• In the majority of PRT drives the LIM or Synchronous Linear Motors (SLM) are adapted (both solutions are equal in terms of technological and exploitation parameters).
• However in the majority of papers, application of LIM as simpler construction cooperating with chipper and easy to make armature is suggested.

For practical realization of PRT drive the one-sided induction motor with inductor placed on vehicle and double layer or ladder secondary (called a reaction plate) on track was chosen. It fulfils basic traction requirements and presents a convenient model for testing supply, control and logistic systems in the laboratory conditions.

Basic design-calculation work concerned realization of down-scaled (in proportion 1:4) SIL prototype models.

In the elaborated calculation methods concerning both the design of construction and also exploitation characteristics the ability of its adaptation to full-scale chosen type SIL was taken in to account. Adaptation was also considered while the technology for work-out of model prototypes, design and work-out of measurement systems and rules of conducting the experiments was decided.

Basic constructional data of motor laboratory model

The value of alternate current linear motor is simple way of progressive electromagnetic field creation, that constitute attribute of its operation, which synchronous velocity is expressed by equation (1) depending on frequency of supply voltage and dimension of pole pitch determined by winding distribution:

$$(1) \qquad v_s = 2f\tau$$

where: f is the supply voltage frequency, τ is pole pitch conditioned by inductor length and pole number.

Advantage of this motor is the technological simplicity and construction of secondary circuit being a track, made of thin layer of good conductivity material (copper, aluminium) placed on only slightly thicker layer of ferromagnetic material. If the winding is placed in the inductor groves the linear induction motor with monolithic secondary is the simplest construction of unique variety and range of application comparing to the other appliances in all techno-sphere.

The main exploitation quantity is the driving force that depends on surface dimension of inductor, that is constituted by number of poles p, pole pitch and inductor width L_i, air gap flux density B_m and current load A_m. This quantity is described as follow:

$$(2) \qquad F_c = k\,p\,\tau\,L_i\,A_m\,B_m$$

Basic kinematics, dynamic and constructional assumptions of full-scale motor for PRT application is collected in Table 1.

In consequence it is possible to determine initially the range of basic overall dimensions and basic nominal exploitation parameters and structural parameters (e.g. winding parameters) of motor.

Table 1. Basic dynamic parameters of full-scale PRT

SYMBOL	QUANTITY	PARAMETER
ε	1,7	Starting overload coefficient
η_m	0,75	Mechanical efficiency coefficient of drive
C	0,5	Aerodynamic drag coefficient
m	1000 [kg]	Vehicle mass with 4 passengers
V	12 [m/s]	Velocity between stops (43,2km/h)
a	1,2 [m/s^2]	Starting acceleration of vehicle
a_n	4 [N/kN]	Rolling resistance of traction roller coefficient
F_a	1,2 [kN]	Acceleration resistance $F_a = m \cdot a$ [kg·m/s^2]
F_A	337,5 [N]	Areodynamic drag $F_A = C \cdot A \cdot (V + V_w)^2$
F_t	40 [N]	Mechanical rolling resistance $F_t = m \cdot g \cdot a_n$
F_w	25,8 [kN]	Total border vehicle movement resistance
P_w	27,5 [kW]	Starting power on the wheels $P_w = F_w \cdot V_a / \eta_m$
P_c	$\approx$ 16 [kW]	Electrical power of vehicle motors $P_c = P_W / \varepsilon$
P_c	$\approx$ 10 [kW]	Motor power in „low land" version

It is necessary to turn attention that it is possible to apply in PRT the autonomous contactless electrical supply traction system (for example in the form of stationary high frequency primary voltage rail next being transformed to the converter circuit of vehicle motor. This allow settling motor voltage, current and frequency nominal value different from these quantities value while supplying from common energy system. For laboratory model of motor, 1:4 down-scaled in respect to full-scale motor the nominal voltage and frequency equal to entry standard values are adapted.

Chosen parameters of motor model determined on the base of similarity rules procedure, but also by conditions of laboratory track are presented in Tab.2.

Table 2. Basic electric, kinetic, and dimensional parameters of motor laboratory model

Description	Symbol	Value
Drive force	Fc [N]	110
Velocity	Vn [m/s]	3,4
Nominal voltage.	U_N [V]	230
Frequency	f [Hz]	50
Inductor width	L_i [mm]	65
Inductor length	L_t [mm]	270
Mechanical gap	g_m [mm]	3,0
Armature thickness	d_{Al} [mm]	2,0

On the stage of preliminary project, taking in to account dimensional limitations of motor model and recommended quantities of exploitation parameters for linear motors (e.g. nominal slip, current density), the next set of output parameters for motor calculation models was determined.

Table 3. Basic preliminary structural and dimensional parameters of motor laboratory model

Nominal slip	s_N	0,25
Phase number	m	3
Pole pair number	p	3
Groves per pole number	q	1
Winding layers number	w	2
Current density	J [A/mm2]	5,0
Groves number.	Q	21
Tooth width	d_z [mm]	6,0
Grove width	d_Q [m]	9,0
Yoke height	h_j [mm]	18,2

Inductor construction

Preliminary determined geometric motor parameters are the basis for formulation of parameterized models for electromagnetic quantities calculation. These models included two subsystem inductors and secondarys being part of race.

Inductor core (Fig.1) is defined by dimensions: length L_{tt}<370 mm and width L_i<70 mm of core pack, yoke height h_j, tooth height h_Q, grove pitch τ_g, tooth width b_Q.
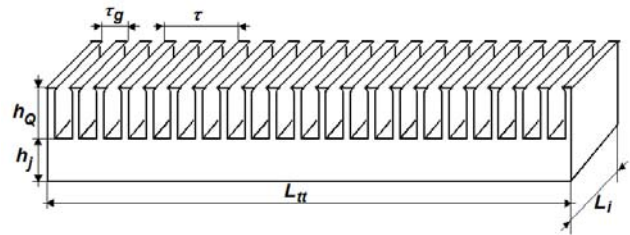
Fig.1. Inductor core with marked cardinal dimensions

Winding

Inductor winding (Fig.14) is determined as six pair of poles $p/2$=6, two layers w=2 with number of groves per pole and phase q=1 and number of groves in the active zone Q=21.

Secondary construction

Secondary (Fig.2) is made as two layers: ferromagnetic core being bottom layer together with cover aluminum plate along all length of track.
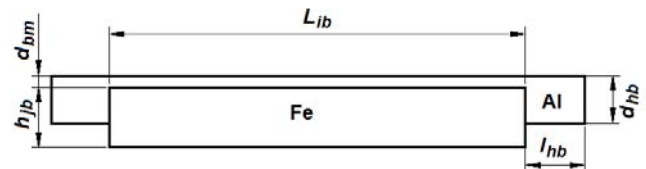
Fig.2. Cross-section of motor secondary

Thickness of ferromagnetic layer h_{bj}>5 mm, conducting layer d_{bm}>2 mm, width of secondary $L_{ib}+2l_{hb}$<150 mm.

For laboratory model LIM the thickness of mechanical gap can be adopted in the range of <2 – 4 mm>.

It should be emphasized, that motor with determined geometric dimensions could be modified electromagnetically in respect to for example number of pair of poles, winding parameters – pitch, number of layers and coil turn number. It is expected to combine inductor with super-structured cooling system with forced medium circulation.

Circuit – field methods of SIL design

Project of motor is calculated on the base of two models – field one concerning electromagnetic quantities in purpose to determine accurate core dimensions and magnetic field distribution in individual elements of magnetic circuit and circuit one in purpose to determine circuit parameters of motor, forces and exploitation characteristics. Calculation of forces (driving and normal) should be mutually verified. Some parameters determined in the course of calculations on the base of both models are mutually used. In the first stage of calculations the circuit model was used and correction of calculations was made on the basis of field model.

Papers [4, 5, 6] are basic positions concerning circuit-field methods of different types of LIM design. Extension of the subject offers study [11].

Circuit method

Below the outline of exemplary algorithm of LIM laboratory model design for nominal operation point "N" is presented. Design procedure accepts double layer and ladder secondary. The last one is considered to use in the start and breaking area of vehicle PRT operation. Subsequent diagram presents main elements of algorithm of operational characteristics and parameters set of LIM determined in previous step essential for control system. Proposed algorithms are based on concept presented in

paper [16]. In the studies [13, 14] of authors of presented paper discussed algorithm is widely extended and universalized.

Start

Postulated among others:
F_C nominal driver force.
v_N nominal velocity.

Material/magnetic data among others:
γ_{Al}, Cu, Fe, C_{WAl}, Cu, Fe,
$B(H)$ characteristic
B_j – joke flux density

Electrical data/dimensions among others:
m, U_{phN}, f, p, q, w, a_g, J,
L_t – induktor width., g_m, d_{Al}, k_{zt}

Calculation:
τ, L_t, t, d_z, d_o, ...

Adoption $N_c = 1$
- initial number of turns in coil

Calculation/Correction
$N_1 = wpqN_c / a_g$

Initial adoption
$0 < \eta \cdot \cos\varphi < 1$

Estimation
$I_1' = F_C v_N / (3 U_{phN} \eta \cos\varphi)$

Calculation:
S_{Cuz}, S_Q, h_Q, k_q, ...

Calculation of equivalent circuit parameters:
R_1, X_1, X_m, $R_2'(s)$, Z
and: $\cos\varphi_o'$, I_1, I_m,
$F_{Co} = m I_2'^2 R'_{2sN}/(v_s s_N)$,
P_m, $P_{el} = P_m + P_{Cu1+2}$,
η_o, $\eta_o \cos\varphi_o$

If $\eta_o' \cos\varphi_o' \approx \eta \cos\varphi$
with precision e.g. 2% — **NO** / **YES**

$\eta \cos\varphi = 0.5 \, (\eta_o' \cos\varphi_o' + \eta \cos\varphi)$

$F_C \approx F_{Co}$ — **NO** / **YES**

$N_c = N_c + 1$

Aditional calculations:
$B_{\delta sr} = f(.. N_1, I_m, k_q, g_m, k_c, d_{Al}, p,.)$
B_z, Φ, U_1, $h_j(B_j)$, J_o, $k_E = U_1 / U_N$
M_{Fe}, M_{Cu}, M, P_{Fe}, η_o, $k_{ef} = F_{Co} / M$
$\lambda_N = F_{Co} / F_{Cmax}$, $\lambda_r = F_{Cor} / F_{Co}$
$F_{nac} = 0.25 \, (d_2 B_2)^2 L_i L_t / (\mu_0 t^2)$

Verification of U_N and calculation of I
$U_{phobl} = abs \, [(R_1 + jX_1) \cdot I_{1c} + jX_{mc}]$
$\delta_{Ujh} \, [\%] = 100 \, abs \, (U_{phobl} - U_{phN}) / U_{phN}$
$I_{mpp} = (\pi B_{\delta sr} \frac{g_e}{\mu_0} + 2H_j h_Q + k_{j1} \tau H_{jg} + SNSB) \frac{\pi p}{2m\sqrt{2} N_1 k_w}$
$\delta I_m \, [\%] = 100 \, abs \, (I_m - I_{mpp}) / I_{mpp}$

END

$s = s_{pocz}$

$s = s + \Delta s$

$R_2'(s)$ - different calculations for two layers secondary

$Z_c(s) = R_1 + jX_1 + \dfrac{j \left[\dfrac{R_2'(s)}{s} \cdot X_m \right]}{\dfrac{R_2'(s)}{s} + jX_m}$

$\cos\varphi_0(s) = Re[Z_c(s)] / abs[Z_c(s)]$

$I_{1c}(s) = U_{phN} / Z_c(s)$

$I_1(s) = abs[I_{1c}(s)]$

$I_{mc}(s) = [U_{phN} - (R_1 + jX_1) \cdot I_{1c}(s)] / jX_m$

$I_m(s) = abs[I_{mc}(s)]$

$I_2'(s) = [X_m \cdot I_m(s) \cdot s] / R_2'(s)$

$v = v_s (1 - s)$

$F_{co}(s) = m \cdot R_2'(s) \cdot [I_2'(s)]^2 / (v_s \cdot s)$

$P_m(s) = F_{co}(s) \cdot v$

$P_{el}(s) = P_m(s) + m\{R_1 \cdot [I_1(s)]^2 + R_2'(s) \cdot [I_2'(s)]^2\}$

$\eta_o(s) = P_m(s) / P_{el}(s)$

$k_{en}(s) = \eta_o(s) \cdot \cos\varphi_0(s)$

$s = s_{end}$ — **NO** / **YES**

END

Basic symbols meaning in the above diagrams:
Fc [N] assumed driving force, F_{co} [N] - calculated driving force, F_n [N] - magnetic pull, V_n [m/s] - assumed and calculated linear velocity, s_n [-] - assumed nominal slip, s [-] - slip – actual value, g_m [mm] - mechanical gap, d_{Al} [mm] - secondary thickness, U_{phn} [V] - supply voltage, f [Hz] - frequency, m - number of phases (in the considered project - 3), p - number of pole pairs of winding, q - number of groves per pole and phase, W - number of winding layers, η - efficiency, $\cos\varphi$ - power factor, $\eta\cos\varphi$ - energetic coefficient SIL, P_m [W] - mechanical power, P_{el} [W] - electrical power, I_1 [A] - supply current, L_t [mm] - inductor length, L_i [mm] - inductor width, h_i [mm] - inductor height, h_j [mm] - inductor yoke height, M [kg] - inductor mass.

General structure of calculations algorithm of LIM project for PRT model for nominal point of operation "N" in steady state is presented on the block diagram above. The characteristic feature of this algorithm is adaptation in the initial data set constant, postulated mechanical parameters: nominal drive force Fc, nominal linear velocity V_N and some magnetic parameters e.g.: flux density in the inductor joke B_j. In the iteration loops of algorithm (appointed by bold block frames), such a value of inductor winding turn N_1 is searched for which calculated values of drive force Fc and energetic coefficient $\eta\cos\varphi$ are equal to the assumed values.

Outline of proposed calculation algorithm of LIM exploitation characteristics: Fc, Pm, Pel, I_1, $\cos\varphi$, η , $\eta\cos\varphi$ = f(V), f(s) presents next block diagram (symbol description above).

Presented algorithms allow for variant project calculation of LIM parameter and exploitation characteristics determination not only for two kinds of secondary but also for different inductor winding structures and mechanical gap thickness between primary and secondary.

Detailed structure of block diagrams, precise discussion of LIM project calculation algorithms, formulas and descriptions are subject of documentation: [8, 9, 13, 14] for double layer and ladder type secondary member.

Field method
Finite element method (FEM) of determination of magnetic field distribution is widely applied, algorithmically reliable and useful for wide range of electrical machines states of operation: steady states dynamic states with DC and AC current and voltage inputs. Modeling and numerical field calculations of presented LIM project was realized using FEM OPERA-2D 2005 version. Parameterized field 2D model of motor was elaborated using Matlab tool program that cooperates with FEM.
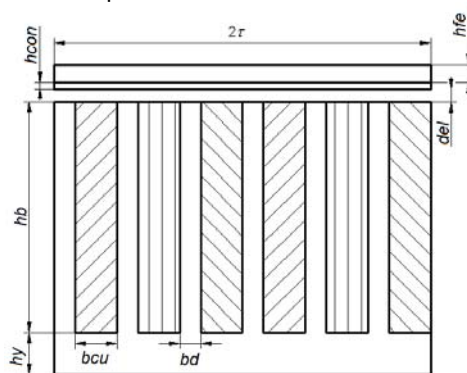
Fig.3. Simplified LIM field model with description of geometric dimensions

First simplified LIM model represents fragment of real object including longitudal cross-section of two pole pitches (Fig.3). Symbol description: hy – yoke thickness (10mm), hb – inductor tooth height, equal to inductor grove depth (55mm), bd – inductor tooth width (5mm), bcu – inductor

grove width (10mm), *del* – air gap thickness (3mm), *hcon* – conductor layer thickness – solid secondary winding (2,5mm), *hfe* – secondary ferromagnetic layer thickness (5mm), 2*τ* – two pole pitches of modeled motor.
Model doesn't take in to consideration parasitic end effects.

Second, more precise LIM model presented on figure 4 and figure 5 with different secondary takes more exactly in to account electromagnetic processes and secondary geometry due to including end effects.
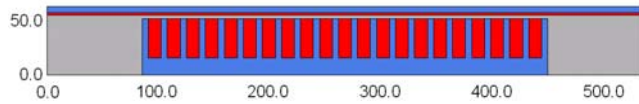
Fig.4. Single sided induction motor with solid secondary
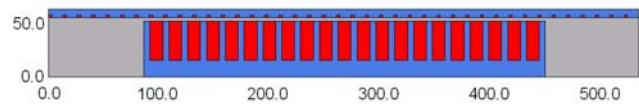
Fig.5. Single sided induction motor with ladder-type secondary

Results of LIM project construction and characteristics calculations

Initial decisions and calculations results in the presented below end set of constructional, exploitation and dimensional parameters of LIM.

Table 4. Set of end constructional exploitation and dimensional parameters of LIM

Description	Symbol	Quantity
Driving force	Fc [N]	110
Velocity	Vn [m/s]	3,37
Nominal voltage	U_N [V]	230
Frequency	f [Hz]	50
Nominal slip	sn	0,25
Phase number	m	3
Pole pair number	p	3
Number of groves per pole	q	1
Number of winding layers	w	2
Current density	J [A/mm2]	5,0
Inductor width	Li [mm]	65
Inductor length	Lt [mm]	270
Mechanical gap	gm [mm]	3,0
Secondary's thickness	dAl [mm]	2,0
Yoke height	hj [mm]	18,2
Grove depth	hQ [mm]	25,5
Tooth width	dz [mm]	6,0
Grove width	dQ [m]	9,0
Turn number	$N1$	654
Number of groves	Q	21

Results that verify those calculations, a part of nominal quantities are exploitation characteristics: mechanical and current ones in respect to velocity. Interesting calculation results is dependence of driving force and normal forces in respect to slip (Fig.6.). Characteristic is alternate monotonicity of driving and normal forces in respect to velocity. Hence in the starting state driving force surpasses normal force, in the nominal speed operation normal force is dominating.
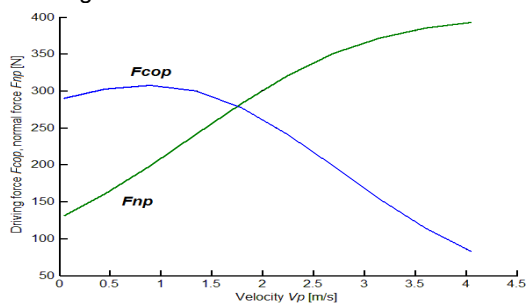
Fig.6. Driving force *Fcop* and normal force *Fnp* characteristic in respect to velocity
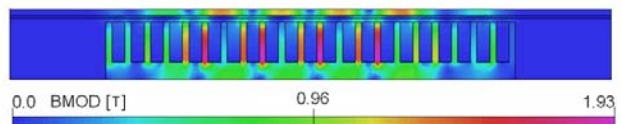
Fig.7. Flux density module In the inductor area

Exemplary results of numerical calculations are presented on figure 7 and figure 8.
Presented below calculated flux density distribution in the air-gap along inductor (Fig.8) is compatible with classic theory of linear induction motors.
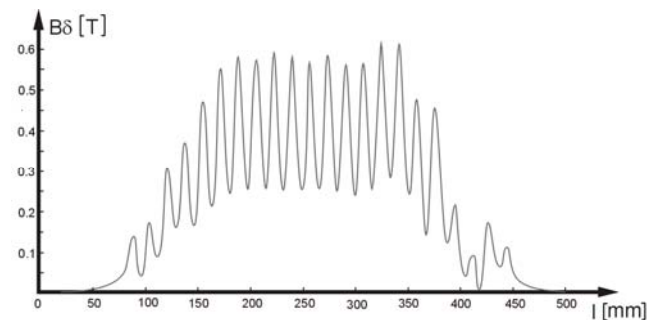
Fig.8. Flux density amplitude distribution In the air gap

It has to be noticed that presented characteristics, maps of distributions and courses of field quantities are exemplary results of whole series of calculations performed for different exploitation and constructional parameters e.g. current, velocity, tooth-grove structure of primary and secondary. Some calculation results e.g. flux density are used in circuit method calculations.

On the figure 9 and figure 10 results of driving force calculations in the full range of LIM line velocity (from start to no load state) on the base of field and circuit model are presented.

Table 4. Basic final exploitation and construction al parameters of LIM design

	Description	Symbol	Quantity
Postulated data	Driving force	Fc [N]	130
	Velocity	Vn [m/s]	3,37
	Slip	sn	0,25
	Secondary's thickness	dAl [mm]	2,0
	Supply voltage	$Uphn$ [V]	230
	Frequency	f [Hz]	45
	Phase number	m	3
	Pole pair number	p	3
	Winding layer number	w	2
	Groves number	Q	21
	Mechanical gap	gm [mm]	3,0
	Inductor width	Li [mm]	65
	Inductor length	Lt [mm]	366
	Inductor height	hi [mm]	65
Results	Driving force	Fco [N]	132
	Normal force	Fn	379
	Number of coil turns	Nc	70
	Number of turns in phase belt	$N1$	420
	Mechanical power	Pm [W]	446
	Eficiency	η [-]	0.45
	Power factor	$\cos\varphi$ [-]	0.14
	Energetic coefficient	$\eta\cos\varphi$ [-]	0.10
	Supply current	I_1 [A]	10
	Inductor width	Lt [mm]	366
	Inductor height	hi [mm]	62,8
	Yoke height	hj [mm]	30,2
	Inductor mass	M [kg]	10.37

Difference of LIM driving force values according to both methods doesn't exceed 30%, what shows correctness of assumed structures of both models.
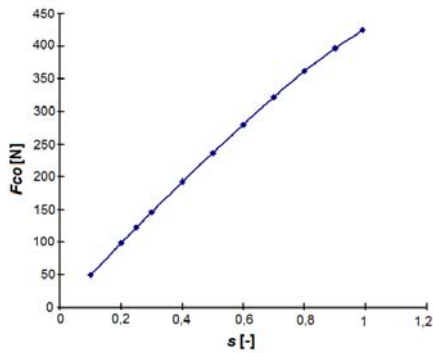
Fig.9. Mechanical characteristic calculated on the base of discrete field model
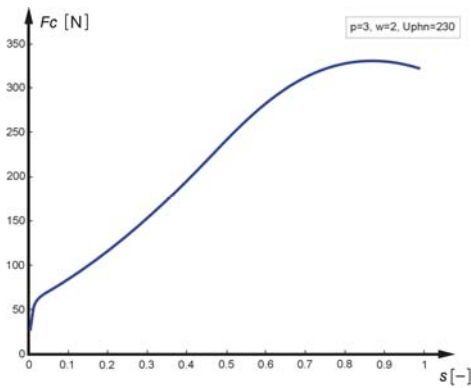
Fig.10. Mechanical characteristic calculated on the base of circuit model
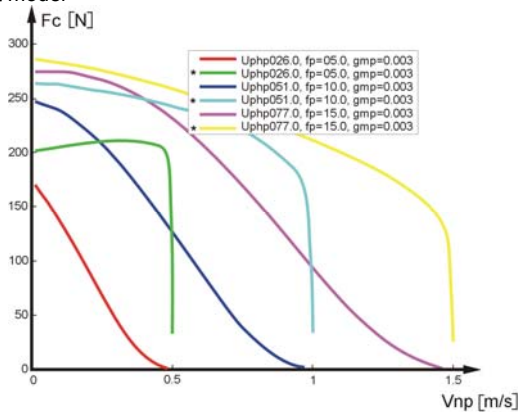
Fig.11. LIM mechanical characteristics for aluminum ladder type secondary, frequency parameterized
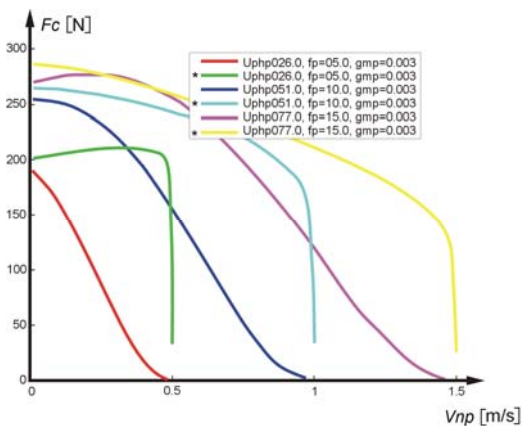
Fig.12. LIM mechanical characteristics for copper ladder type secondary, frequency parameterized

Important results of calculations are self dependencies constructional-exploitation that constitute basis of choice of construction and motor control rules. Exemplary self dependencies are functions of drive and normal force and current in respect to supply voltage or voltage frequency or mechanical characteristics determined for different secondary constructions. For proposed construction of ladder type secondary the comparative LIM mechanical characteristics of layer type secondary for full spectrum of supply voltage frequencies f=5, 10, 15, 20, 30, 45 Hz while keeping constant U/f ratio were calculated. Exemplary calculation results for two types of ladder type secondary (Al, Cu) in comparison to layer type secondary (mark with asterisk) for chosen supply voltage frequency as a function of mover velocity are presented on figure 11 and figure 12. Characteristics are calculated for constant voltage to frequency ratio.

Presented characteristics reveals that calculation model for ladder type secondary structure is low sensitive to material parameters, as their driving forces values differs only insignificantly. These calculations shows also that ladder type secondary don't cause, apart of few local points, increase of driving force comparing to layer type secondary. It has to be stated that experimental results shows significant advantage of ladder type secondary over layer type secondary particularly in the range of low velocities and low frequencies values. This is important due to possible decrease of starting currents of motor with ladder type secondary.

Construction and technology of LIM laboratory model

On the base of project and parametric calculations the linear motor construction consists of one sided inductor and two types of secondary was elaborated. Inductor construction was arranged to be placed on vehicle and controlled by frequency converter. Secondary choice was determined by regarding economic aspect and effectiveness of vehicle dynamics. Ladder type secondary is destined for stops and turnout track part [7, 8, 9].

Construction and technology of motor inductor

The main linear motor constructional parts are inductor core and winding (Fig.13, Fig.14) and reaction plate.

Induction core is made of packed electro-technical metal sheets welded along external joke surface. In the core pack there are holes that serve for motor fixing to the PRT vehicle according to documentation of Transport Department, Warsaw University of technology project group.
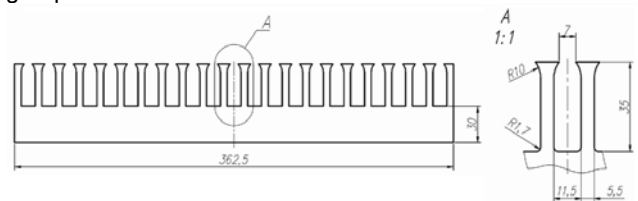
Fig.13. Metal sheet of magnetic core
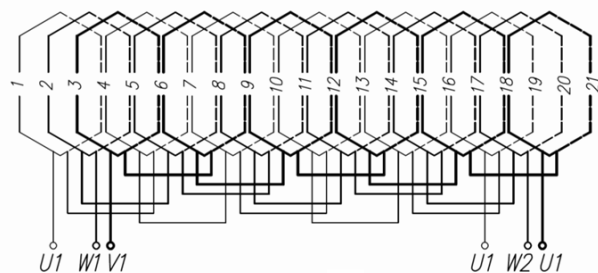
Coil: 70 turns 2xDNE ⌀0,80
Fig.14. LIM compact inductor winding diagram

Fifteen groves of conductor core is filled with two layers and six with one layer winding. The winding area is equipped with 2 – 4 thermocouples. After groves closing with wedges and head part of winding bandaged, inductor was drying in the temperature 120°C during 12 hours with aim to remove all humidity prior to winding impregnation (Fig.15).
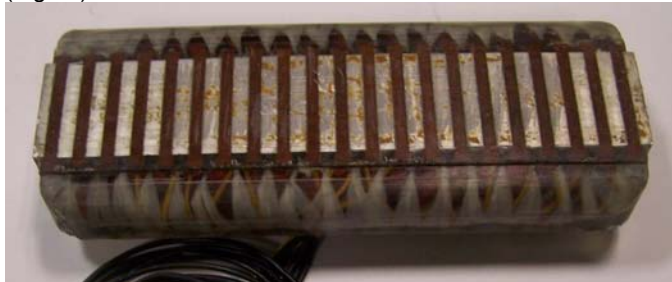
Fig.15. View of inductor with impregnated winding

Fig.16. Layer type secondary a) copper, b) aluminum
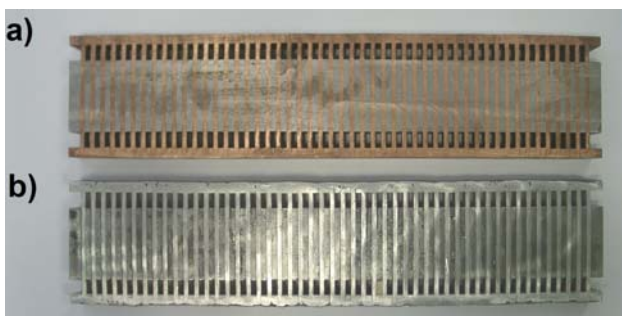
Fig.17. Ladder type secondary with: a) copper bars, b) aluminum bars

For laboratory testing two basic types of secondary: layer and ladder types were made (Fig.16). Layer type secondary was equipped with copper and aluminum conductor plate. To the secondary ferromagnetic layer the conductor cover plate was fixed using bolt joints.

Two versions of ladder type secondary was made: with short-circuited copper and aluminum winding. Both bars and short-circuited rails are made of copper and aluminum respectively (Fig.17). Bars and rails are welded using hard solder.

Methods of experimental tests and measurement system

Experimental test of progressive movement motors concerning full kinematics range are highly complicated. Comparatively easy are tests in inductor locked state. Difficulty of experimental tests also relates instrumental part covering supply sources, measurement sensors and converters and data acquisition system. Problem of supply sources is linked with wide measurement range requiring current, voltage and velocity changes. For parametric setting of these quantities it is necessary to dispose of voltage source with independent voltage RMS, and frequency regulation. Substantial difficulty in synonymous

determination of voltage or current is content of higher frequency harmonics. Specifically difficult are dynamic state measurements of these motors, hence for evaluation of its dynamics it is necessary to develop new test methods.

Having this in mind experimental tests of linear motors require special measurement tools that secure measurement precision, tests universality and efficiency. Only high class sensors and converters and data processing systems could be up to these requirements. That why applying of CAM techniques supplemented with virtual measurement technology is indispensable.

For electromagnetic driving and normal forces measurement the special platform equipped with force sensors is designed and worked out (Fig.18).

Fig.18. Device for driving and normal forces measurement

Chosen test results of LIM model experimental test

Experimental test are the final stage of work concerning new constructions of electrical machines, that allow to verify correctness of motor carry-out and assembling, symmetry of motor circuits, correctness of project calculations and determination of circuit parameters. The aim of tests is also evaluation of movement and kinematics properties of designed motor.
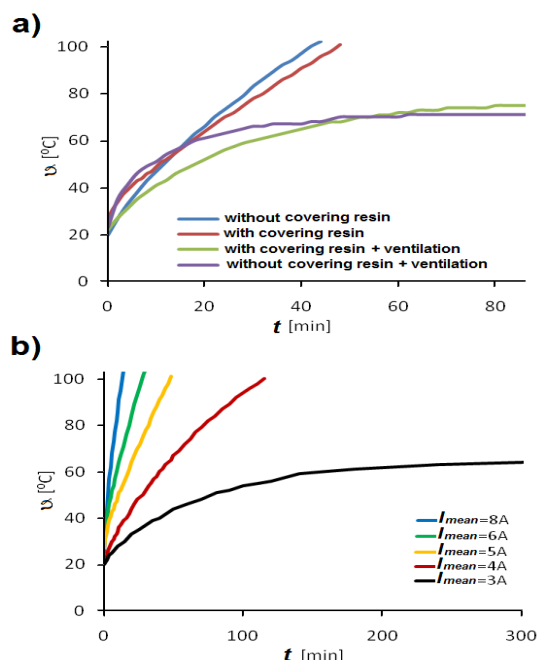
Fig.19. Heating curves of LIM: a) in the different cooling conditions (I = 5 A), b) compact version for different winding current

Thermal tests

The first stage of experimental tests was temperature measurements (Fig.19), that allow estimating permissible currents in short-circuited state of operation (starting state).

It is worthy to notice, that winding impregnation and covering with epoxide resin results in increasing of temperature time constant (Fig.19a) of inductor and decreasing of allowable uninterruptible operation current. That means that from one side the ability of instantaneous LIM overload increase, from the other the mean load value decreases.

On Fig.19b the heating curves for the winding part that is most thermally loaded is presented. As it results from graphs motor circuit characterizes the temperature time constant of several minutes rank, what allows for instantaneous increase of driving force above nominal values. The substantial current increase (up to 10 A) could effect in exceeding allowable temperature for given insulation class in several minutes.

In this stage a great amount of heat is emitted in the secondary, what because of comparatively small thermal capacity results much higher temperature rise that in the inductor windings. That means that the range of force operation e.g. in stationary inductor position has to be limited to short time intervals or small current loads.

a)

b)
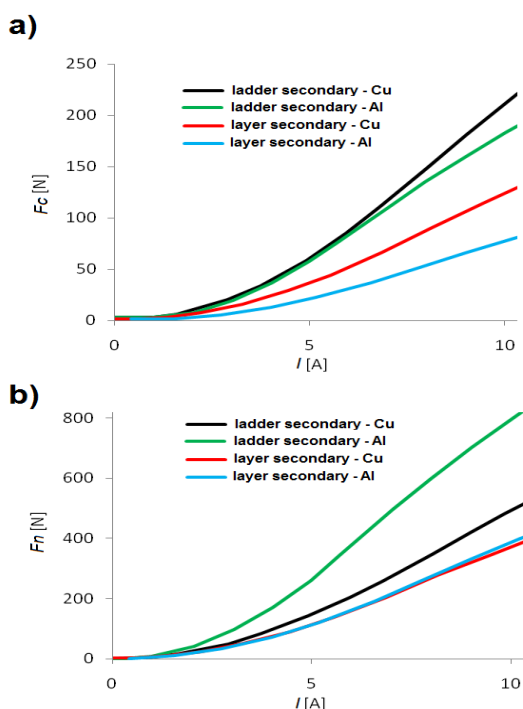
Fig.20. Dependence of driving and normal forces generated by LIM in the steady state of operation as a function of current for supply voltage frequency f = 10 Hz

Force measurement

Wide range of experimental tests concerned also measurements of driving and normal forces in respect to starting process and motor kinematics. For the technical reasons forces were measured only in steady state of operation called short circuit state.

According to experiment schedule firstly the measurements were performed in respect to supply voltage level. Voltage as a rule determines electromagnetic reaction (forces and torques) in electrical machines. Determined characteristics (Fig.20) are presented as a function of current, because of ability to more precise determination of current RMS value peculiarly while supplying voltage from frequency converter. Presented characteristics shows parabolic dependence of forces on voltages what is compliant with calculation model of LIMs (for linear dependence of voltages and currents).

Important results of experimental tests concern dependence of driving force as a function of frequency for constant current values for different secondary types.
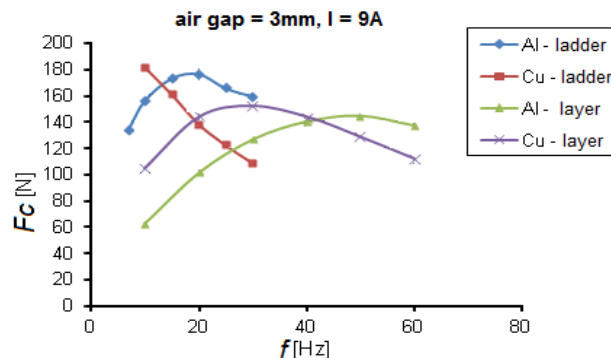
Fig.21. Dependence of driving force on frequency for different types of secondary

Particularly important is extreme driving force for ladder type secondary with copper bars for low frequency (starting frequency) (Fig.21). This was indicated also in the calculation results, however less significant. This supports postulate of introduction this kind of secondary in the PRT stop area.

Flux density measurements

The aim of flux density measurements in the air gap of LIM is determination of its mean value and modification of space harmonics of time sequence. Determination of those values allows for verification project calculations.

Among many ways of determining space flux density distribution the method based on periodicity of time sequence presented in paper [10] is applied. On the figure 22 the flux density distribution in the air gap along inductor for two values of supply current is presented. From maximal values of flux density follows that tooth-grove area of inductor in magnetized in small degree. That implies possibility of decreasing teeth width and increasing of groves mmf by increasing phase coils turn number.
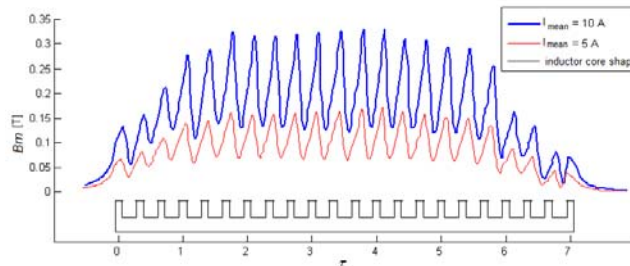
Fig.22. Envelope of flux density distribution in the LIM air gap in the steady state of operation

Testing of of LIM laboratory model in dynamic state of operation

Within the limit of experimental tests the kinematics tests includes movement of one of motor models along short track. The aim of those tests was to determine current values during reverse state of operation and limited dynamics estimation. During tests mass of motor was changed. Kinematic experiment performed on limited track length (about 6 m) requires special security system, which performs motor reverse and constant control of electrical and kinematic parameters. For purpose of full observation of movement the frequency and supply voltage was limited to f=10 Hz and U=60 V. Result of experiment was elaborated in form of graphs: displacement, velocity and acceleration (driving force) and movement trajectory in coordinates a = f(v).

On figure 23 and figure 24 the graphs of displacement, velocity, acceleration and phase portrait of velocity and acceleration in the reversal machine movement are presented. It should be stated that original measurement signal is distorted by noise created by frequency converter. So for determination of secondary signals there is necessary to perform filtering using specially adopted average moving filters.
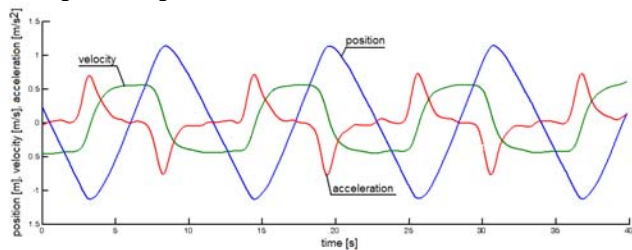
Fig.23. Graphs of displacement, velocity and acceleration of LIM model in reverse movement regime of operation
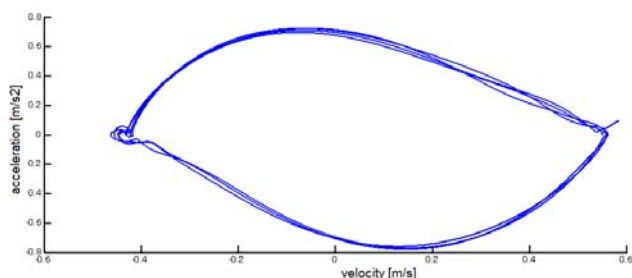
Fig.24. Phase portrait of velocity and acceleration of LIM model in reverse movement regime of operation

As it results from measured values of velocity and acceleration which is the measure of driving force, motor features good dynamics because for increased mass and substantially decreased supply voltage in respect to nominal voltage it achieves 0,3 of nominal velocity and driving force equal to half of nominal one for three times lower current. It is necessary to state that current fluctuation in reversal movement differs comparing to mean value by about 2%.

Conclusions

• Performed excessive tests confirm sufficient level of conformity between calculated and postulated parameters of down scaled LIM model of different constructions.

• Applied calculation and design hybrid methods prove to be effective and are not time consuming.

• Used algorithms can be easy adopted for full scale LIM design

Authors: *prof. dr hab. inż. Grzegorz Kamiński, Politechnika Warszawska, Instytut Sterowania i Elektroniki Przemysłowej, ul. Koszykowa 75, 00-662 Warszawa, E-mail: g.kaminski@ime.pw.edu.pl; dr hab. inż. Włodzimierz Przyborowski, Instytut Sterowania i Elektroniki Przemysłowej, ul. Koszykowa 75, 00-662 Warszawa, E-mail: W.Przyborowski@ime.pw.edu.pl; prof. dr hab. inż. Paweł Staszewski, Politechnika Warszawska, Instytut Sterowania i Elektroniki Przemysłowej, ul. Koszykowa 75, 00-662 Warszawa, E-mail: staszew2@yahoo.pl; dr inż. Adam Biernat, Instytut Sterowania i Elektroniki Przemysłowej, ul. Koszykowa 75, 00-662 Warszawa, E-mail: adam.biernat@ee.pw.edu.pl; mgr inż. Emil Kupiec, Instytut Sterowania i Elektroniki Przemysłowej, ul. Koszykowa 75, 00-662 Warszawa, E-mail: kupiece@ee.pw.edu.pl;*

REFERENCES

[1] Anderson J. E., High-Capacity Personal Rapid Transit: Rationale, Attributes, Status, Economics, Benefits, and Courses of Study for Engineers and Planners, 2007
[2] Anderson J. E., The Future of High-Capacity Personal Rapid Transit, PRT International, LLC, Minneapolis, Minnesota, USA, November 2005
[3] Bishop R. H., Learning with LabVIEW 8TM , ISBN 0-13239025-6, PEARSON Prentice Hall, 2007
[4] Gieras J., Silniki Indukcyjne Liniowe, ISBN 83-204-1116-5, WNT Warszawa, 1990.
[5] Gieras J. F., Piech Z.J.: Linear synchronous motors, Transporattion and automation systems, CRC Press LLC, Boca Raton, London, New York, Washington 2000.
[6] Gieras J. F., Linear Induction Drives, 1994
[7] Kamiński G., Projekt ,konstrukcja ,technologia silnika liniowego.Opracowanie wewnętrzne ZME 2010.
[8] Kamiński G., Przyborowski W., Staszewski P., Biernat A., Kupiec E.: Badania laboratoryjne SIL do napędu modelu PRT. Etap 2: Badania laboratoryjne SIL z bieżnią warstwową i wstępna analiza porównawcza z wynikami obliczeń. Raport wewnętrzny z prac zrealizowanych w Projekcie Eco-Mobilność, UD/0092/1160/2011.
[9] Kamiński G., Przyborowski W., Staszewski P., Biernat A., Kupiec E., Rogalski A.: Projekt uzwojenia dwuzwojnego, wykonanie wzbudnika z tym uzwojeniem i wykonanie stanowiska do badań eksperymentalnych modelu SIL napędu PRT z jednoczesnym pomiarem siły ciągu i naciągu oraz minimalizacją tarcia ruchu bieżnika. Raport wewnętrzny z prac zrealizowanych w Projekcie Eco-Mobilność, nr UD/1160/E0084/6/101, 2012
[10] Kupiec E., Przyborowski W.: Metoda wyznaczania i analiza rozkładu indukcji magnetycznej w szczelinie powietrznej silnika indukcyjnego liniowego. Zeszyty Problemowe – Maszyny Elektryczne nr 100 cz. 2, 2013, BOBREM Komel, s. 121-126.
[11] Lu G., Li Q., Liu Z., Fan Y. and Li G.: The Analytical Calculation of the Thrust and Normal Force and Force Analyses for Linear Induction Motor, ICSP 2008 Proceedings, 2008
[12] Nasar S.A.: Handbook of Electric Machines, New York, McGraw-Hill Book Company, 1987.
[13] Przyborowski W., Staszewski P., Herbst A.: Projekt SIL do napędu modeli PRT metodą obwodową z uwzględnieniem bieżni drabinkowej oraz wyznaczenie charakterystyk pracy i zbioru parametrów niezbędnych do układów sterowania. Etap 2: Projekt SIL z bieżnią drabinkową do napędu modelu PRT oraz wyznaczenie podstawowych parametrów elektromechanicznych i charakterystyk pracy. Raport wewnętrzny z prac zrealizowanych w Projekcie Eco-Mobilność, nr UD/0000/1160/2010
[14] Przyborowski W., Staszewski P., Herbst A.: Projekt SIL do napędu modeli PRT metodą obwodową z uwzględnieniem bieżni drabinkowej oraz wyznaczenie charakterystyk pracy i zbioru parametrów niezbędnych do układów sterowania. Etap 1: Wyznaczenie charakterystyk pracy i zbioru parametrów do układu sterowania zaprojektowanej konstrukcji SIL z bieżnią warstwową w zależności od parametrów zasilania i szczeliny mechanicznej. Raport wewnętrzny z prac zrealizowanych w Projekcie Eco-Mobilność, nr UD/0000/1160/2010 ©.
[15] Ranky P.G.: Magne Motion's linear synchronous motor (LSM) driven assembly automation and material handling system designs, Assembly Automation, Volume 27, Number 2, 2007.
[16] Sarveswara-Prasad-Bhamidi: Design of a Single Sided Linear Induction Motor (SLIM) Using a User Interactive Computer Program, University of Missouri-Columbia, Thesis, May 2005.
[17] Yamamura S., Ono E.: Linear synchronous motor, Report 371 of the General Meeting, IEE Japan, Tokyo Section, 1967.